Mon. Not. R. Astron. Soc. **319**, 419–428 (2000)

Detailed visual observations and modelling of the 1998 Leonid shower

P. Brown[1,2]★ and R. Arlt[2]

[1]*Department of Physics and Astronomy, University of Western Ontario, London, Ontario, N6A 3K7 Canada*
[2]*International Meteor Organization, PF 600118, D-14401 Potsdam, Germany*

Accepted 2000 May 8. Received 2000 May 8; in original form 2000 February 11

ABSTRACT

We present a detailed activity profile for the 1998 Leonid shower from visual observations. The shower displayed at least two distinct components – a broad component peaking between 234°.4 and 235°.0, and two narrower filaments near 235°.21 and 235°.33 probably of younger origin based on modelling results. This dual-peaked structure in the flux profile has peak fluxes to a limiting magnitude of +6.5 of 0.03 Leonid $km^{-2} h^{-1}$. The distribution of particles also changes dramatically across the stream in 1998, with large meteoroids dominating the early peak and smaller meteoroids relatively more abundant near the time of the nodal passage of the comet. Detailed comparison of the observed activity with models in 1998 shows that the early component comes from material ejected between 500 and 1000 yr ago. Our modelling results suggest that the later dual peaks are caused by high-β meteoroids with large ejection velocities released during the 1932 and 1965 passages of Comet 55P/Tempel–Tuttle.

Key words: comets: individual: 55P/Tempel–Tuttle – meteors, meteoroids.

1 INTRODUCTION

The Leonid shower is the strongest of the periodic showers currently visible at Earth. Approximately every 33.3 yr the shower increases dramatically in activity and may produce one or more meteor storms. One such storm has already been witnessed in 1999 (Arlt et al. 1999).

Detailed observational histories of Leonid storms have been published in many references (e.g. Yeomans 1981; Mason 1995; Brown 1999). As rich as the history of the observation of the stream has been, the history of the attempts to understand its origin and evolution and ultimately to make predictions about its possible future activity is equally rich.

While predictions varied as to the strength and duration expected of the shower in 1998 (e.g. Mason 1995), no advanced warning from any source was given concerning the spectacular early 'fireball' peak widely recorded some 20 h before the crossing of the nodal plane of 55P/Tempel–Tuttle (e.g. Arlt 1998). A secondary peak was recorded shortly after the nodal passage, weaker in activity than the early peak and shorter in duration.

Asher, Bailey & Emel'yanenko (1999) have shown convincingly that the mechanism responsible for the early fireball peak is the 'resonant protection' of low-β Leonids associated with the 5:14 resonance with Jupiter. This mechanism concentrates old ejections by allowing daughter meteoroids from 55P/Tempel–Tuttle to remain in the Jovian 5:14 with the parent comet and thus disperse in semimajor axis much more slowly than would otherwise be the case. However, ongoing dispersion in the ascending node and nodal radii of the resonant population does occur, with the resulting activity far below that of recent ejections where the spatial density is orders of magnitude greater.

Here we present detailed results of visual observations of the 1998 shower with emphasis on the substructures visible in the flux and particle distribution profiles. We compare these results with detailed modelling of the 1998 shower to determine age and possible ejection conditions for both the early fireball peak and the later nodal peak. The visual observations consist of some 70 800 Leonids recorded by 473 observers in 43 countries during the period 1998 November 3–29. Total effective observing time for this study was 2171 h. The source for all visual data was the Visual Meteor Database (VMDB) maintained by the International Meteor Organization (IMO) (e.g. Arlt 1999).

2 VISUAL RESULTS

2.1 Magnitude distributions

The methods used to collect and analyse visual data follow the standards established by the IMO [see Rendtel, Arlt & McBeath (1995) for a detailed description]. For the present study only Leonid magnitude distributions are selected for the determination of population indices r which fulfil four criteria.

(i) At least five consecutive magnitude classes should be involved in the resulting r-value.

(ii) The faintest of these magnitude classes should be more than

★ E-mail: pbrown@julian.uwo.ca

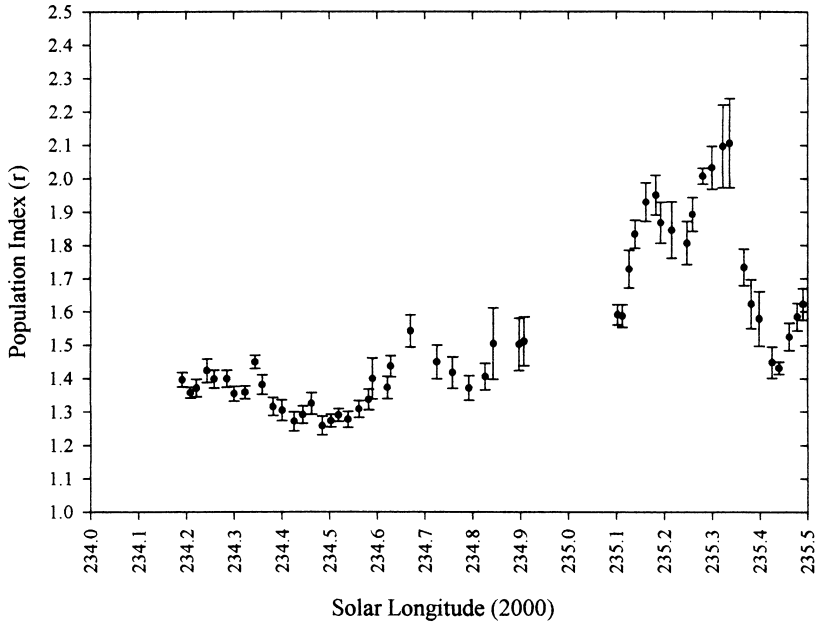

Figure 1. High-resolution profile of the population index r of the 1998 Leonids covering the period of highest activity.

Table 1. Bin sizes for the population index profile in Fig. 1.

Range in $\lambda_\odot$	Bin width	Shift
234.°18–234.°60	0.°04	0.°02
234.°60–234.°86	0.°08	0.°04
234.°86–235.°12	0.°20	0.°10
235.°12–235.°50	0.°04	0.°02

2 mag from the stellar limiting magnitude, because the probability of detecting a meteor is extremely low near the limiting magnitude, and small meteor numbers seen by the observer will be corrected to very large true meteor numbers, thus introducing large errors.

(iii) The total number of meteors in the magnitude distribution should be equal to or larger than 20. This figure has been found empirically to be the minimum useful for a single measure of the population index.

(iv) The true number of meteors in each magnitude class (i.e. meteor number seen corrected with the perception probability) is larger than 3.0.

The perception probabilities have been taken from meteors recorded in 'double-count' observations, where two observers face fixed parts of the sky and note the relative positions of meteors. Fig. 1 shows the population index profile between November 16, 18:00 and November 18, 0:50 UT. There are three local maxima visible in this graph: the first during the fireball peak near $\lambda_\odot = 234.°67 \pm 0.°05$, another just before the nodal peak at $\lambda_\odot = 235.°18 \pm 0.°04$ and the most distinct local maximum close to the nodal passage of 55P/Tempel–Tuttle at $\lambda_\odot = 235.°34 \pm 0.°01$. Here the population index r refers to the ratio $N(M+1)/N(M)$, where M is the meteor magnitude and $N(M)$ the true number of meteors recorded in the Mth magnitude interval. The bin sizes used for the calculation of the population index are given in Table 1.

The calculation of the population index assumes that the cumulative number of shower meteors versus the magnitude follows an exponential distribution characterized by a single

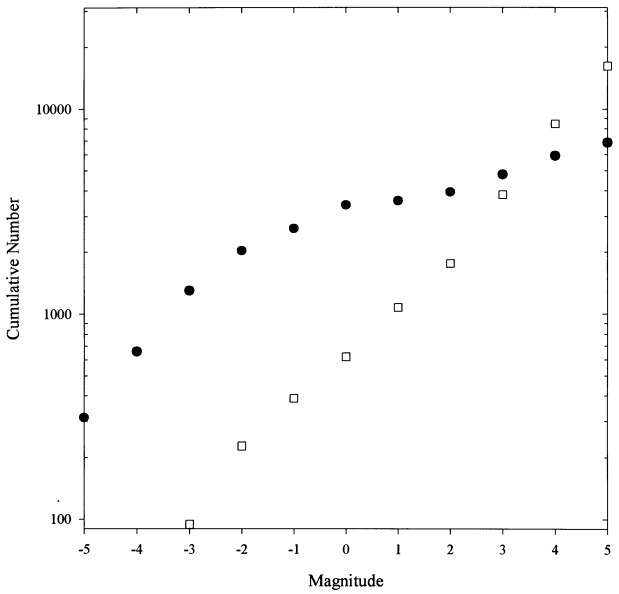

Figure 2. Cumulative magnitude distribution for all Leonids recorded between $\lambda_\odot = 234.°0$ and $235.°0$ (filled circles) and from $\lambda_\odot = 235.°0$ to $235.°5$ (open squares).

exponent. An exponential distribution delivers the same linear slope ($\log r$ for cumulative and non-cumulative distributions if the number of meteors is large). Fig. 2 shows the logarithmic cumulative magnitude distribution for Leonids in the interval of the fireball maximum (solid circles) and the regular maximum near the nodal passage of 55P/Tempel–Tuttle (open squares) for all observations with limiting magnitudes of +6.0 or better. Note that the observed numbers of Leonids have been corrected for the perception probability in each magnitude class (cf. Rendtel et al. 1995). The former distribution is clearly not a single exponential distribution over the entire magnitude range shown – specific r-values derived over this interval are not quantitatively meaningful. During the fireball maximum the particle mass distribution

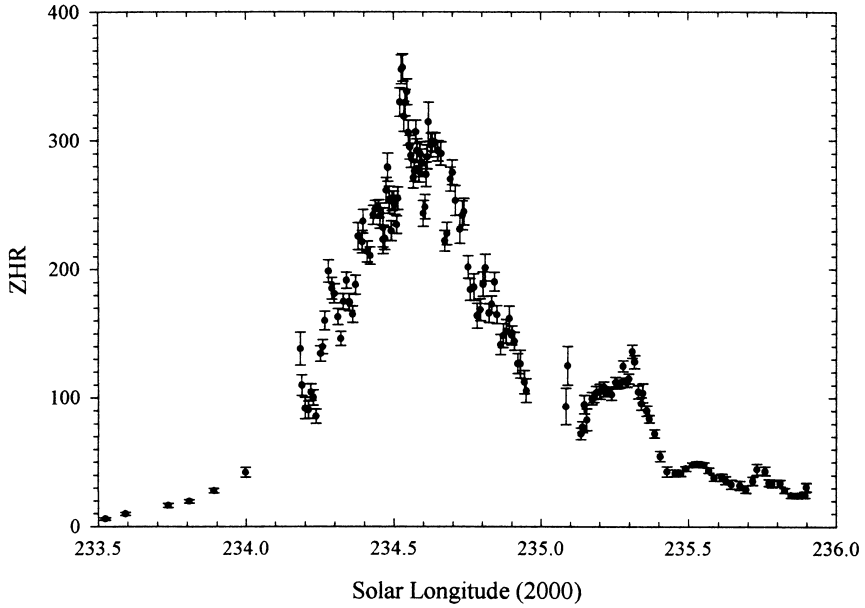

Figure 3. The ZHR profile of the 1998 Leonids from $\lambda_\odot = 233^\circ.5$ to $236^\circ.0$.

appears to deviate from an exponential for equivalent magnitudes brighter than +2. The enhancement in moderately bright Leonids (near −2 to −3) is more than an order of magnitude greater as compared with the period near the nodal maximum (where $r \approx 1.8$ fits the distribution well over the entire magnitude range).

2.2 The ZHR profile

The first step in computing the zenithal hourly rate (ZHR) is determining the population index profile, as was done above. Observers' shower meteor numbers are then corrected according to their stellar limiting magnitudes to the standard magnitude of +6.5. The high-resolution graph of Fig. 1 might reflect spurious, statistical variations on to the ZHR profile; we therefore applied a coarser population index profile for the computation of the ZHR. The window size for this smooth *r*-profile was $0^\circ.2$ shifted by $0^\circ.1$. Two selection criteria were applied to all individual ZHR values before they were to be used in the final averages:

(i) minimum radiant elevation of 20°;

(ii) maximum correction factor $r^{(6.5-lm)}F/\sin h_R < 5$, where *lm* is the stellar limiting magnitude, *F* is a factor for possible obstructions of the field of view, and h_R is the radiant elevation.

It is not an easy task to find the optimum bin size for averaging a quantity like the ZHR. Large bins may suppress short-lived structures in the time series; small bins may produce much larger error bars than the fluctuations that they reveal, and the profile will tend to be less reliable. The choice of bin size corresponds directly with the spectral content allowed through into the resulting profile. Thus quoting a value for the ZHR is meaningless unless some indication of the filtering used on the profile (through choice of bin size and averaging step) is also given.

The ZHR profile for the entire period of significant activity (November 15–18) of the Leonids in 1998 is given in Fig. 3. Table 2 provides the binning intervals and windowing used to construct the graph.

The ZHR profile during the time of the fireball 'maximum' (November 16) is shown in Fig. 4, while that near the nodal maximum is shown in Fig. 5. In 1998, the ZHR maximum occurs

Table 2. Bin sizes for the ZHR profile in Fig. 3.

Range in $\lambda_\odot$	Bin width	Shift
$232^\circ.00$	$2^\circ.00$	$1^\circ.000$
$232^\circ.00$–$234^\circ.10$	$0^\circ.20$	$0^\circ.100$
$234^\circ.10$–$234^\circ.46$	$0^\circ.04$	$0^\circ.020$
$234^\circ.46$–$234^\circ.62$	$0^\circ.01$	$0^\circ.005$
$234^\circ.62$–$235^\circ.35$	$0^\circ.02$	$0^\circ.010$
$235^\circ.35$–$236^\circ.00$	$0^\circ.04$	$0^\circ.020$
$236^\circ.00$	$1^\circ.00$	$0^\circ.500$

at $\lambda_\odot = 234^\circ.53 \pm 0^\circ.01$ with a magnitude of 357 ± 11. From Fig. 4 it is evident that a significant number of additional sub-maxima in the ZHR profile occur in the region of the fireball peak, most notably near $\lambda_\odot = 234^\circ.28$, $234^\circ.4$, $234^\circ.48$, 23462, $234^\circ.7$ and $234^\circ.81$. However, when the number of observers contributing data in each interval is examined, it becomes clear that some of these peaks may be observational artefacts. In particular, we note that minima (with fewer than 15 observers contributing) in the number of observers used per interval (the sizes of which are given in Table 1) are found in the regions near $\lambda_\odot = 234^\circ.28$, $234^\circ.38$, $234^\circ.46$, $234^\circ.62$, $234^\circ.71$ and $234^\circ.78$.

The correlation of these observer minima with the ZHR maxima casts doubt on the significance of some of these features, as the relative paucity of observers in these solar longitude intervals may produce a small systematic increase in the ZHR relative to neighbouring intervals. The overall full width to half-maximum for the fireball peak is found to be in the range 11–13 h; this duration corresponds to a thickness for this stream component perpendicular to the orbital plane of approximately 4×10^5 km. The period near the nodal maximum is shown in Fig. 5 with the location of the peak at $\lambda_\odot = 234^\circ.31 \pm 0^\circ.01$ with a magnitude of 136 ± 5. Comparing the location of this maximum with the *r*-profile in Fig. 1, we find that the location of maximum coincides almost directly with the maximum in the population index, with a difference of 40 min between the times of the two maxima. The ZHR profile is best described as flat from $\lambda_\odot = 235^\circ.3$ to $235^\circ.3$ with a near-constant value of 100–110.

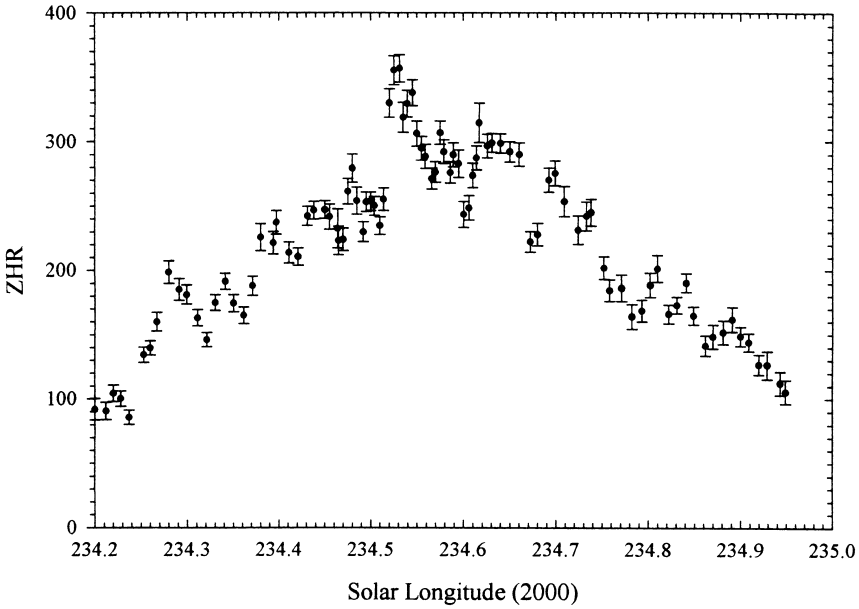

Figure 4. The ZHR profile of the 1998 Leonids centred about the fireball peak.

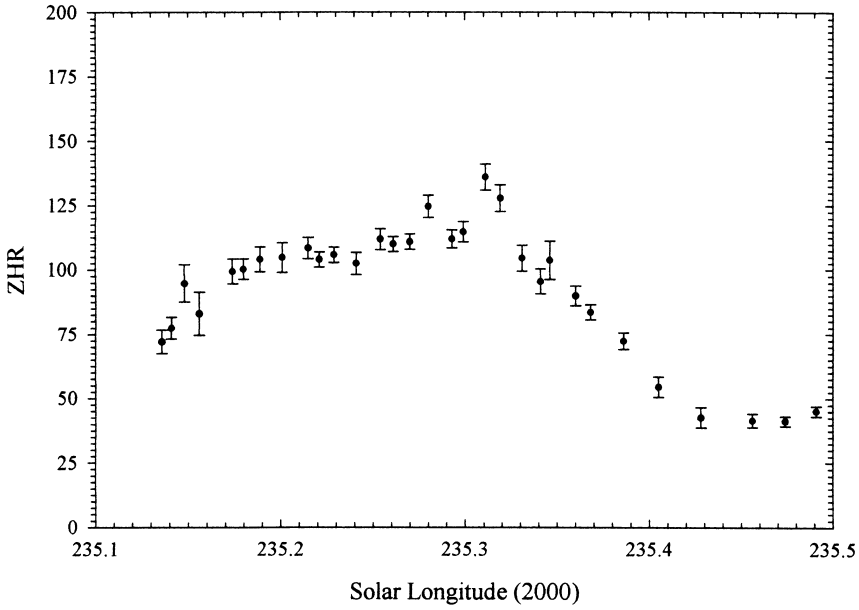

Figure 5. The ZHR profile of the 1998 Leonids centred about the nodal peak.

2.3 Flux

By using the population index and ZHR measures together, we are able to derive an absolute influx of Leonids above a specified magnitude threshold. Details for the calculation of flux are given in Brown & Rendtel (1996) and Arlt (1998).

As the fireball peak and nodal peak have dramatically different particle populations, we show flux calculated at three differing absolute magnitude levels. Fig. 6 shows the flux at three different magnitude thresholds. The top panel is for very bright Leonids ($M_{V\mathrm{abs}} \geq -4$ or mass ≥ 1 g), the middle panel for medium visual brightness Leonids ($M_{V\mathrm{abs}} \geq +3$ or mass $\geq 10^{-3}$ g) and the bottom panel for Leonids with $M_{V\mathrm{abs}} \geq +6.5$ or mass $\geq 2 \times 10^{-5}$ g. As expected, the fireball maximum completely dominates the flux at the largest masses, while extension to the smallest masses makes the nodal peak dominant.

Heuristically this can be understood from the fact that the effective collecting area in the atmosphere for visual observers is much larger for brighter meteors (as during the night of the fireball peak), and this is what causes the integrated flux at the smallest masses to be modest at the time of the fireball maximum (in contrast to the much smaller collecting areas during the nodal peak when r was higher). Most notable is the pronounced double maximum near the time of the nodal peak at the smallest masses, a feature not typically found in other shower profiles (see Rendtel et al. 1995). Fig. 7 shows the flux in this solar longitude range in greater detail. The first maximum occurs at $\lambda_{\odot} = 235\overset{\circ}{.}21 \pm 0\overset{\circ}{.}02$ and is followed by a pronounced minimum occurring at

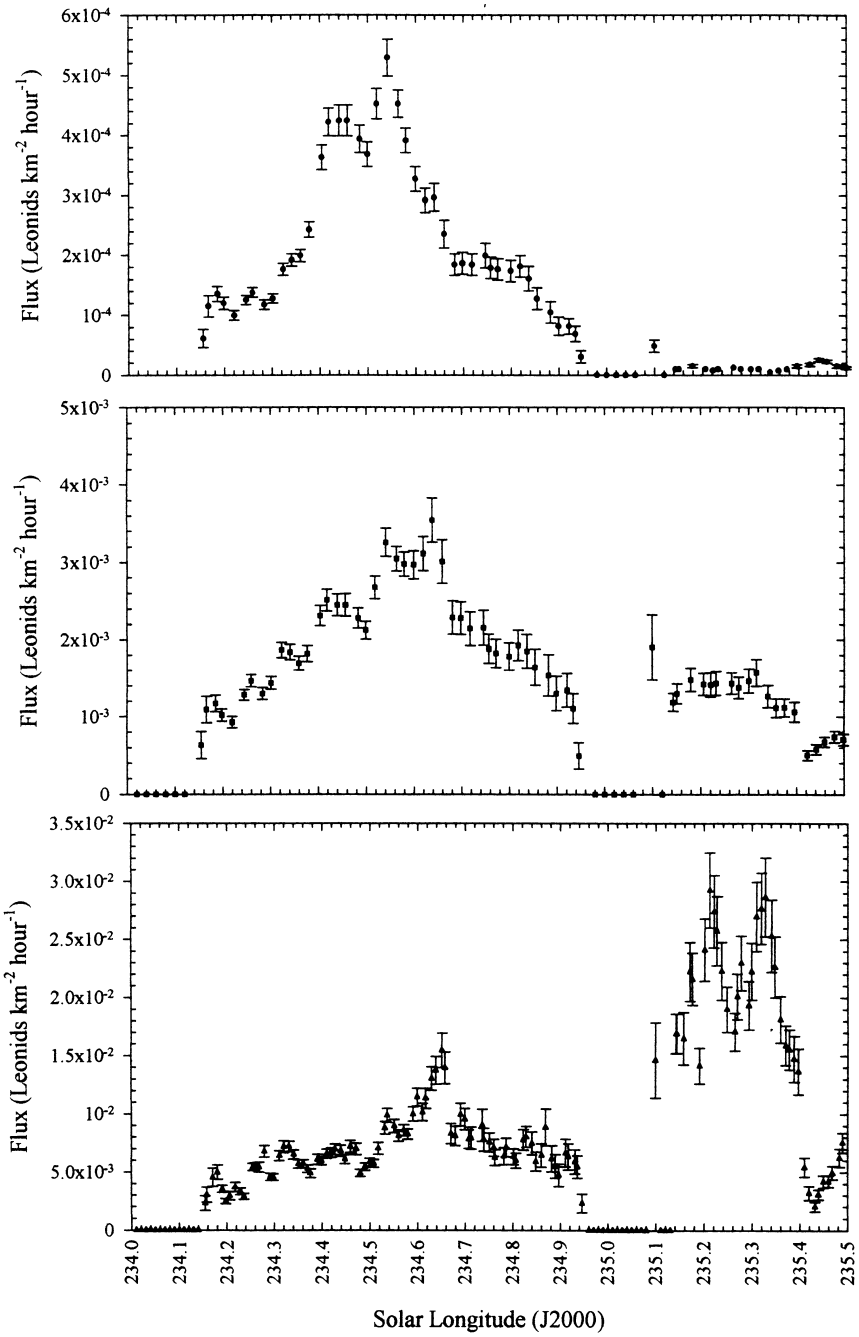

Figure 6. The flux profile of the Leonids at three threshold sizes: for Leonids with $M_{V\mathrm{abs}} \geq -4$ (top), $M_{V\mathrm{abs}} \geq +3$ (middle) and $M_{V\mathrm{abs}} \geq +6.5$ (bottom).

$\lambda_\odot = 235\overset{\circ}{.}26 \pm 0\overset{\circ}{.}01$, the present nodal position of 55P/Tempel–Tuttle. The second maximum occurs at $\lambda_\odot = 235\overset{\circ}{.}33 \pm 0\overset{\circ}{.}01$. It is probable that this structure is the direct result of the change in the population index (see Fig. 1) across this solar longitude range, and hints directly at two different (recent) ejection origins for these two maxima.

3 MODELLING THE 1998 LEONID SHOWER

3.1 Overview of model

To examine the Leonid material enountered by the Earth in 1998, we have used the output of a numerical model which consists of generating a suite of test particles close to each perihelion passage of 55P/Tempel–Tuttle and following each of these through to the epoch of interest. 'Daughter' Leonids were created through random ejection on the sunward hemisphere of 55P/Tempel–Tuttle, and were distributed at random in true anomaly inside 4 au. The osculating elements for 55P/Tempel–Tuttle were taken from Yeomans, Yau & Weissman (1996). A total of 10 000 test meteoroids were ejected in each decadal mass interval from 10 to 10^{-5} g, for a total per perihelion passage of 70 000 test particles. This procedure was repeated for each of the last 15 perihelion passages of the comet so that each complete 'run' consists of almost 1 million test particles. In addition to these 500 year-long 'runs', a single run spanning 2000 yr was performed for one model

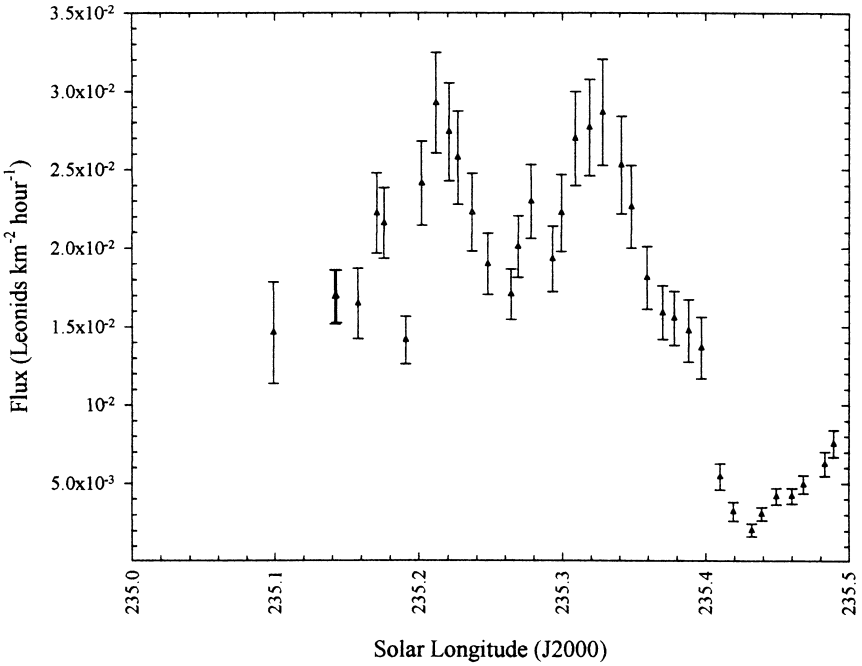

Figure 7. The flux profile of the Leonids near the time of the nodal maximum for Leonids with $M_{V\mathrm{abs}} \geq +6.5$.

to examine effects of older ejections on the 1998 shower. For the 2000-yr run (composed of 57 perihelion passages), the ejection velocities are given by the modified Whipple formula (e.g. Brown & Jones, 1998) as

$$V_{\mathrm{eject}} = 10.2 r^{-0.5} \rho^{-1/3} R_{\mathrm{c}}^{0.5} m^{-1/6}, \quad (1)$$

where r is the heliocentric distance at the time of ejection in au, ρ is the bulk density in g cm^{-3}, R_{c} is the cometary radius in km, and m is the mass of the particle in g.

After the initial conditions were specified in this way, each test particle was numerically integrated forward from ejection to the epoch of interest and followed until it reached its descending node and its Keplerian elements at the time of nodal passage were stored. The integration included the direct and indirect perturbations of all planets from Venus to Neptune, radiation pressure and the Poynting–Robertson effect. The integrator used was a fourth-order variable-step-size Runge–Kutta (Jones 1985).

This basic procedure was repeated for four different physical models of ejection and three different values of meteoroid bulk density for a total of 12 different runs. The four physical models were derived from the work of Crifo (1995) on distributed gas production within the cometary coma, and the Jones (1995) model with variations in the heliocentric dependence on ejection velocity and a parabolic distribution in meteoroid ejection probabilities. For each of these models we adopted bulk meteoroid densities of 0.1, 0.8 and 4.0 g cm^{-3} in turn, owing to uncertainties in the actual meteoroid bulk density, and in order to investigate the role of differing assumed densities on the evolution of the stream. These densities, along with the range in initial particle masses, translate into a range of β from 10^{-5} to 10^{-2}.

Our approach is to generate initial conditions that are 'reasonable' within the constraints of our imperfect understanding of the cometary coma dust environment, rather than to suggest any particular model as most appropriate. In particular, we recognize there to be large uncertainties in many of the physical quantities (i.e. density of meteoroids, relationship between meteoroid mass and luminosity, etc.), and choose instead to explore the effects of widely different (but still 'reasonable') ejection conditions (velocities, points of ejection and ejection directions) and meteoroid densities over a wide range of masses in this Monte Carlo fashion. This same approach has been used previously to study the formation and evolution of the Perseid stream (Brown & Jones 1998), and more extensive details and discussion can be found in that work. Our hope is to identify effects insensitive to initial conditions and thus likely to be true features of the stream.

3.2 Results for 1998

All material ejected with nodal passage times within 1 week of the shower in 1998 were classified as possible Leonids. The nodal distances for each 'streamlet' from all models ejected since 1633 are shown in Fig. 8; the mean nodal distance from the Sun for all particles and the standard deviation of the population are also given. Note that we have summed over all solar longitudes and for all masses from 10^{-3} to 10 g for all models to produce this graph. The size of the standard deviation gives a first-order estimate of the sunward extension of each streamlet per model. As can be seen from the small difference between each model, the choice of initial ejection velocity distributions has a minor influence over the radial extent of the streamlet.

The location of all these recently produced streamlets in 1998 was considerably sunward of Earth, typically by distances of 0.005–0.008 au. The fact that none of the standard deviations of any model for any streamlet back to 1633 overlaps the Earth suggests that few particles from these ejection epochs would be expected to encounter Earth in 1998, as was observed. In fact, examination of the output from all models shows no significant numbers of Leonids intersecting the Earth back to the longest (500 yr) model runs.

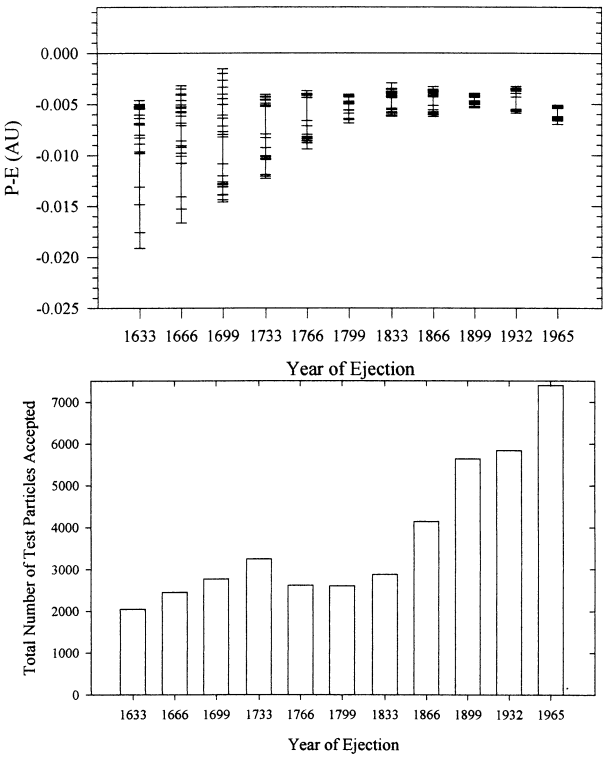

Figure 8. Nodal distance and spreads for each streamlet ejected since 1633 at the time of the 1998 Leonid shower (top), where P-E is the difference between the particle nodal distance and the Earth's nodal distance in au. The plot shows the number of test particles from each ejection epoch with nodal passage times within one week of Earth's passage through the Leonid stream in 1998.

Examination of the longer (2000 yr) runs, however, reveals a population dominated by larger meteoroids originating from ejections in the 500–1000 yr old range and forming the parent population which produced the fireball peak in 1998, and we examine these data next.

3.3 The fireball peak

To examine the model output for the 1998 Leonid fireball peak, we limit our selection of test particles further to only those occurring in the solar longitude interval from $\lambda_\odot = 234\overset{\circ}{.}0$ to $235\overset{\circ}{.}0$. Fig. 9 shows the number of test particles that were within 1 week of nodal passage at the time of the Earth's nodal crossing of 55P/Tempel–Tuttle's orbit in 1998, as well as being spatially within 0.001 au of Earth's orbit for all perihelion passages since 79 AD. Notable is that little recent (less than 500 yr old) material is present, and that the meteoroids appear to originate in ejections that are 500–1000 yr old. We note that no one ejection epoch completely dominates the delivery of material over this solar longitude interval in 1998. We also remark that all the model runs extending back only 500 yr show only small numbers of test particles accepted in 1998, and these are all from the oldest ejections included in those runs. As a result, we confine the remainder of our examination of the fireball peak to the 2000 yr old run.

Fig. 10 shows the distribution by mass as a function of solar longitude for particles accepted in the interval of the fireball peak. It is clear that very large Leonids are preferentially associated with

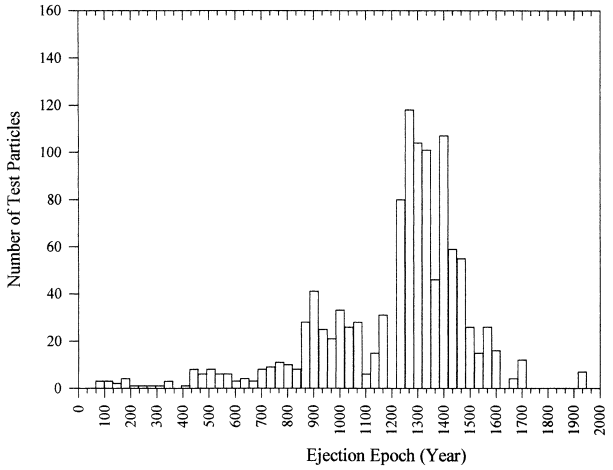

Figure 9. Number of test particles for 1998 Leonids per perihelion passage for meteoroids with $m \geq 10^{-3}$ g.

this solar longitude interval and (from Fig. 9) that these derive from many perihelion passages of 55P/Tempel–Tuttle during the 12th–14th centuries.

Fig. 11 shows the distribution of accepted Leonids as a function of solar longitude and nodal distance. Note that several epochs have many large Leonids contributing to 1998 which originate from ejection near perihelion. It should also be emphasized that the ejection velocity interval sampled here is limited by equation (1) – in particular, the ejection velocities near perihelion are generally above $\sim 10\,\mathrm{m\,s^{-1}}$.

3.4 The nodal peak

From Fig. 9 it is apparent that few particles of recent ejection origin with $\beta \leq 10^{-3}$ come close to Earth's orbit in 1998 using the ejection conditions adopted for the 2000-yr modelling. In particular, the three most recent ejections have most material well inside the Earth's orbit, with large numbers of meteoroids concentrated more than 0.003 au away from Earth's orbit. Of particular interest for the origin of the nodal peak are the three most recent ejections with particles concentrated in the solar longitude interval near $\lambda_\odot = 235\overset{\circ}{.}2$–$235\overset{\circ}{.}4$.

Almost all ejection models used here (with total ejection velocities over $100\,\mathrm{m\,s^{-1}}$ for the smallest particles) produced very little material within 0.001 au. of Earth at the time of the shower in 1998. To decipher further the likely dynamical cause of the nodal peak, we examined the few particles accepted as possible 1998 Leonids from these three ejection intervals.

Of the 840 000 test particles ejected at each perihelion from all 12 models, a total of 0, 15 and 9 test particles ended up within 0.001 au of Earth's orbit and passed through their ascending node within one week of the Earth in 1998 from ejections in 1899, 1932 and 1965 respectively. For these test particles, the ensemble from 1932 had a mean solar longitude at the descending node of $\lambda_\odot = 235\overset{\circ}{.}22 \pm 0\overset{\circ}{.}07$, while those from 1965 were located at $\lambda_\odot = 235\overset{\circ}{.}34 \pm 0\overset{\circ}{.}04$. This immediately suggests a possible linkage of the first flux peak (located at $\lambda_\odot = 235\overset{\circ}{.}21$) with 1932 material and the second flux peak located at $\lambda_\odot = 235\overset{\circ}{.}33$ with 1965 ejecta.

Several ejection origins for this material in 1998 from the simulations are evident. For the 1965 ejecta (associated with the later nodal flux peak), all associated test meteoroids had relatively

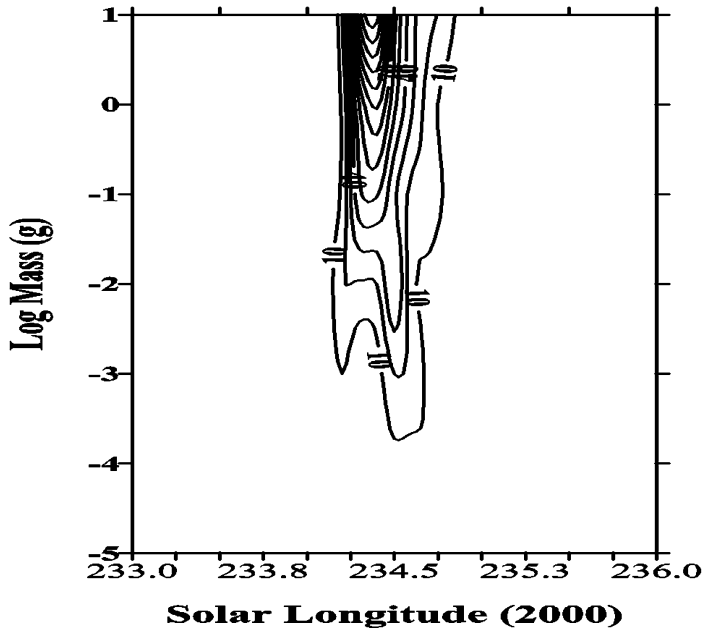

Figure 10. 1998 Leonid test particles by mass as a function of solar longitude for ejections over the last 2000 yr.

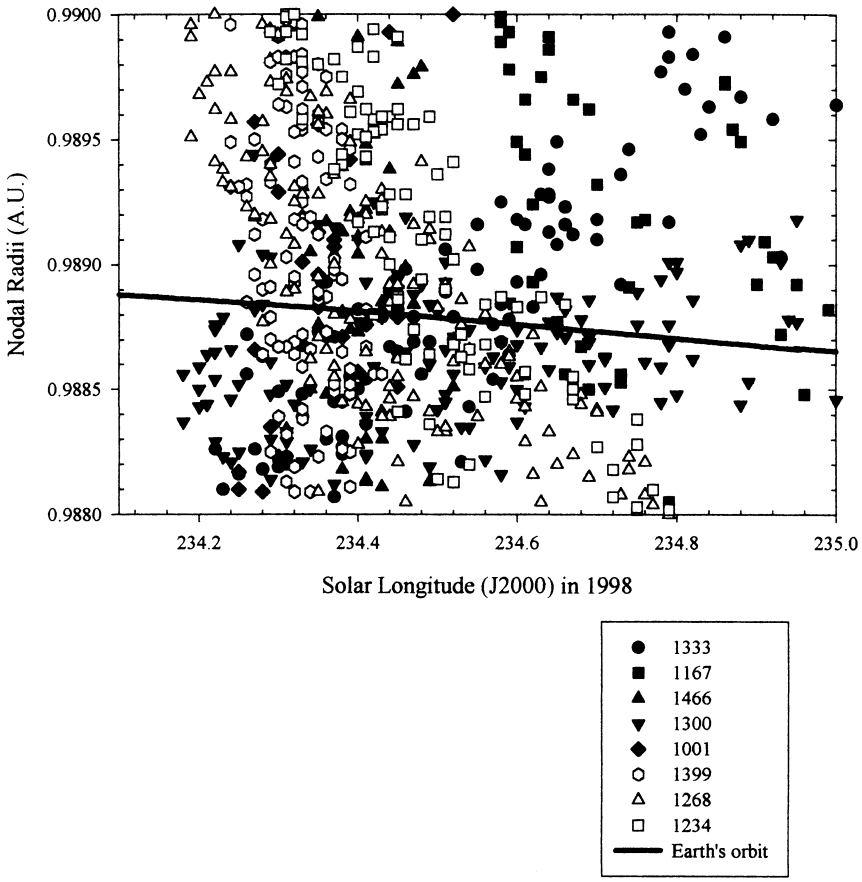

Figure 11. Distribution of nodal distances for test particles with mass = 10 g from several ejection eras (see figure legend) as a function of solar longitude.

large values of β, between 10^{-3} and 9×10^{-3}, with the majority of test particles near 0.004–0.005. Of note is that all accepted Leonids from the 1965 ejection were ejected post-perihelion at a distance of 2.5–4 au from the Sun. The required ejection velocities to make these particles into 1998 Leonids were between 20 and 60 m s^{-1}, with a large positive (i.e. in the direction of the comet's motion) velocity component. The exact ejection velocities, location and associated β were found to be the determining

factors as to whether particles ended up with descending nodal radii near the Earth's orbit at the time of the 1998 shower. In contrast, the action of planetary perturbations was found to be negligible in the delivery of these test meteoroids to nodal distances near Earth's orbit (and at the proper nodal passage time).

For the ejecta from 1932, at least three distinct ejection origins are possible in 1998 for delivery near the nodal peak. First, a similar situation to 1965 ejection is evident, namely particles ejected at large post-perihelion distances (more than 3 au), with values of $\beta = 5 \times 10^{-3}$. Also, several particles with very small $\beta = 5 \times 10^{-5}$ were found to have intersection conditions with Earth in 1998 near later solar longitudes if ejected at almost 4 au pre-perihelion with low velocities (of order 5 m s^{-1}, entirely in the direction of 55P/Tempel–Tuttle's motion. Additionally, a third population ejected just after perihelion (near 1 au) at extremely high velocities (150 m s^{-1} such that the positive transverse velocity component is approximately 80 m s^{-1}) and with very large $\beta = 0.02$ also make it to Earth-crossing at the time of the 1998 Leonids. As with the 1965 ejecta, it was found that planetary perturbations were not significant for delivery; rather, radiation pressure forces and initial ejection conditions controlled evolution to Earth-crossing at the time of the 1998 shower.

4 DISCUSSION AND CONCLUSIONS

From the global visual observations of the 1998 shower presented here, a clear picture of activity having several different ejection origins is apparent.

First, the broad, fireball peak beginning almost 24 h prior to Earth's passage through the nodal longitude of 55P/Tempel–Tuttle is clearly the result of older, large Leonid meteoroids, controlled by the 5:14 resonance as discussed by Asher et al. (1999). Using a modified Whipple ejection velocity scenario, we have shown the material encountered during this broad component to be composed of ejections from many perihelion passages of 55P/Tempel–Tuttle, as opposed to solely from 1333 as proposed by Asher et al. (1999).

To confirm that our results are not simply the product of our initial choice of ejection velocity distribution, we re-ran the ejection simulations from 1200 to 1500 AD for large meteoroids (with $\beta = 0$), and randomly chose ejection velocities between 0 and 20 m s^{-1} inside 2 au. Our results mirrored the earlier larger scale integrations, the four ejections between 1267 and 1367 AD being the most prolific contributors to the activity in 1998, with average solar longitudes for these particles in 1998 near $\lambda_\odot = 234\overset{\circ}{.}50$ and probable ejection velocities from 5 to 20 m s^{-1}. From our earlier results (cf. Fig. 11), ejections outside this period also contribute particles both before and after this solar longitude interval, providing a plausible explaination for the observed long duration of the broad, large-mass Leonid component.

We further note that the population of particles from all of these ejections had average osculating semi-major axis values at their descending nodal passages of 10.36–10.38 au, with very small dispersion in these averages. This is near the average semi-major axis of 10.35 au for the 5:14 resonance (Asher et al. 1999), further confirming this mechanism as the probable cause of the large particle population in 1998.

We also compared these revised integrations with the observational results of Betlem et al. (1999). In particular, we have found that adding ejection epochs other than 1333 broadens the final orbital distribution of particles responsible for the fireball peak. In particular, using only the results of the ejections from 1000 to 1500 AD we find a spread in inclinations from $161\overset{\circ}{.}7$ to $162\overset{\circ}{.}2$ and in the argument of perihelion from $171\overset{\circ}{.}5$ to 172°. As noted by Betlem et al. (1999), the observed orbital distribution from photographic data gathered during the fireball maximum on November 16/17 shows ranges in these elements of $161\overset{\circ}{.}6$–$162\overset{\circ}{.}4$ and $169\overset{\circ}{.}5$–172° respectively. Inclusion of test particles of many differing ages improves the fit between the observed and theoretical spreads (notably in the inclination distribution) in these orbital elements when compared with the single return spread which assumes 1333 as the sole source of the fireball material from Asher et al. (1999). However, some discrepancy (particularly in the argument of perihelion) between our resulting modelled distributions and those observed remains. From the original data given by Betlem et al. (1999), however, all but a handful (four) of the observed Leonids with arguments of perihelion much smaller than the theoretical range have large enough error in ω to overlap our final modelled range in this quantity.

From the visually determined flux, we have resolved the nodal 'peak' into two distinct peaks, centred at $\lambda_\odot = 235\overset{\circ}{.}21 \pm 0\overset{\circ}{.}02$ and a second maximum at $\lambda_\odot = 235\overset{\circ}{.}33 \pm 0\overset{\circ}{.}01$. Jenniskens (1999) examined video flux data in this interval and noted an unusual asymmetric shape to the flux profile (which he found to peak at $\lambda_\odot = 235\overset{\circ}{.}31 \pm 0\overset{\circ}{.}01$). He suggested that this broad asymmetric peak is caused by contributions from two distinct (but in his data unresolved) ejections of recent origins. We find a very similar picture, with the flux profile clearly showing the locations of two distinct peaks, and are able tentatively to match these from modelling with ejecta from 1932 (for the earlier sub-maxima) and 1965 (from the later sub-maxima) based on the solar longitudes of resulting test particles from those epochs.

Additionally, we have found the test particles from 1932 and 1965 to have several possible ejection origins/physical characteristics. All were (generally) found to be high-β meteoroids (from 0.005 to 0.02) and the ejecta from 1965 appears to be associated potentially with more distant post-perihelion activity ($r \geq 2.5$ au) with high ejection velocities. The earlier peak (from 1932 ejecta) was also found to have some test particles with a similar ejection origin as those from 1965. In addition to these, however, some test particles were found to be very high-β particles ejected with exceptionally large velocities (of order 150 m s^{-1}) near perihelion and large meteoroids (with small β) ejected at large distance pre-perihelion.

While any/all of these origins are possible, it is notable that the origins with high velocity, particularly distant ejections (as well as near perihelion for 1932, for example), also cause a large spread in the resulting orbital elements. Indeed, Betlem et al. (1999) remark that the large dispersion in orbital elements from Leonids recorded on the night of 1998 November 17/18 (during the nodal peak) may be ascribed to ejection velocities of order 100 m s^{-1} (assuming an origin 2–4 revolutions in age). This is qualitatively consistent with our findings from modelling, and we suggest by implication that the material associated with the nodal peak in 1998 comprised the 'tail' of the high-velocity, high-β meteoroids released by 55P/Tempel–Tuttle in 1932 and 1965. This picture is also consistent with the relatively weak increase in rates observed near the nodal peak owing to the small number of particles that we would expect to meet this condition, as well as the lack of larger Leonids. While the majority of meteoroids released from 55P/Tempel–Tuttle (even near perihelion) would be expected to have ejection velocities of 10 m s^{-1} [also based on the widths of past observed

Leonids storms from Brown (1999)], unusually shaped objects might well have ejection velocities an order of magnitude greater than the average, as Gustafson (1997) has emphasized.

ACKNOWLEDGMENTS

The authors thank the numerous visual observers who reported their observations to the IMO and thus made a major part of this analysis possible. PB thanks the United States Air Force, the European Space Agency, the Canadian Space Agency, the Canadian Department of National Defence, and Hughes Aerospace for funding assistance.

REFERENCES

Arlt R., 1998, WGN, 26, 239
Arlt R., 1999, in Baggaley W. J., Porubcan V., eds, Meteoroids 1998. Astron. Inst. Slovak Acad. Sci.
Arlt R., Rubio L. B., Brown P., Gyssens M., 1999, WGN, 27, 286
Asher D. J., Bailey M. E., Emel'yanenko V. V., 1999, MNRAS, 304, L53
Betlem H. et al., 1999, Meteorit. Planet. Sci., 34, 979
Brown P., 1999, Icarus, 138, 287
Brown P., Rendtel J., 1996, Icarus, 124, 414
Brown P., Jones J., 1998, Icarus, 133, 36
Crifo J. F., 1995, ApJ, 445, 470
Gustafson B. A. S., 1994, Rev. Planet. Space. Sci.
Jenniskens P., 1999, Meteorit. Planet. Sci., 34, 959
Jones J., 1985, MNRAS, 217, 523
Jones J., 1995, MNRAS, 275, 773
Mason J., 1995, J. Br. Astron. Assoc., 105, 219
Rendtel J., Arlt R., McBeath A., 1995, Handbook for Visual Meteor Observers. IMO, Potsdam, Germany
Yeomans D., 1981, Icarus, 47, 492
Yeomans D., Yau K. K., Weissman P. R., 1996, Icarus, 124, 407

This paper has been typeset from a TEX/LATEX file prepared by the author.